AFRL-OSR-VA-TR-2013-0559

ROLLED-UP OPTICAL AND ELECTRONIC COMPONENTS FOR ON-CHIP INTEGRATIVE APPLICATIONS

OLIVER SCHMIDT

INSTITUTE FOR INTEGRATIVE NANOSCIENCES, IFW DRESDEN

10/10/2013
Final Report

AIR FORCE RESEARCH LABORATORY
AF OFFICE OF SCIENTIFIC RESEARCH (AFOSR)/RSE
ARLINGTON, VIRGINIA 22203
AIR FORCE MATERIEL COMMAND

REPORT DOCUMENTATION PAGE

Form Approved
OMB No. 0704-0188

1. REPORT DATE *(DD-MM-YYYY)*	**2. REPORT TYPE**	**3. DATES COVERED** *(From - To)*
04-10-2013	Final Report	June 2009 - June 2013

4. TITLE AND SUBTITLE

ROLLED-UP OPTICAL AND ELECTRONIC COMPONENTS FOR ON-CHIP INTEGRATIVE APPLICATIONS

5a. CONTRACT NUMBER
FA9550-09-1-0550

5b. GRANT NUMBER

5c. PROGRAM ELEMENT NUMBER

6. AUTHOR(S)

Daniel Grimm; Libo Ma; Matthew Jorgensen R.; Shilong Li; Stefan Böttner; Stefan Harazim; Oliver G. Schmidt

5d. PROJECT NUMBER

5e. TASK NUMBER

5f. WORK UNIT NUMBER

7. PERFORMING ORGANIZATION NAME(S) AND ADDRESS(ES)

IFW-Dresden, Helmholtzstr. 20, 01069 Dresden, Germany

8. PERFORMING ORGANIZATION REPORT NUMBER

9. SPONSORING / MONITORING AGENCY NAME(S) AND ADDRESS(ES)

10. SPONSOR/MONITOR'S ACRONYM(S)

11. SPONSOR/MONITOR'S REPORT NUMBER(S)

12. DISTRIBUTION / AVAILABILITY STATEMENT

13. SUPPLEMENTARY NOTES

14. ABSTRACT

Rolled-up microtube cavities were prepared for optical and electronic applications. For Optical components, the quality factor was greatly improved by introducing an axial confinement. Optical modes tuning was systematically investigated which led to a variety of optical sensing applications, including on-chip integrative microtube resonator for optofluidic sensing, dynamic molecular process sensing, and angular position detection of single nanoparticles. Add-drop configuration in microtube resonator was explored through microcavity-fiber coupling. A novel method for the fabrication of rolled-up diamond lattice photonic crystals was proposed. Finite element calculations support the proposed method. Optical spin-orbit coupling was realized in cone-like microtube cavity, which implies promising applications by manipulating photons in on-chip quantum devices. For electronic components, rolled-up capacitors were fabricated. Compacted metal-oxide field effect transistors withstanding ultra-small bending radii were prepared for integration into microfluidic application as electronic sensing devices.

15. SUBJECT TERMS

Rolled-up microtube; Optical three-dimensional confinement; Optical modes tuning; Optofluidics; Optical sensing; Rolled photoni

16. SECURITY CLASSIFICATION OF:			**17. LIMITATION OF ABSTRACT**	**18. NUMBER OF PAGES**	**19a. NAME OF RESPONSIBLE PERSON**
a. REPORT	**b. ABSTRACT**	**c. THIS PAGE**			Prof. Dr. Oliver G. Schmidt
					19b. TELEPHONE NUMBER *(include area code)* +49-(0)351 4659 800

Report Submission Form

1. Report Type

Final Report

Primary Contact E-mail

Contact email if there is a problem with the report

o.schmidt@ifw-dresden.de

Primary Contact Phone Number

Contact phone number if there is a problem with the report *

+49-(0)351 4659 800

Organization / Institution name

IFW Dresden e.V.

Institute for Integrative Nanosciences

Award Information

Grant/Contract Title

The full title of the funded effort

ROLLED-UP OPTICAL AND ELECTRONIC COMPONENTS FOR ON-CHIP INTEGRATIVE APPLICATIONS

Grant/Contract Number

AFOSR assigned control number. It must begin with "FA9550" or "F49620".

FA9550-09-1-0550

Principal Investigator Name

Prof. Dr. Prof. h.c. Oliver G. Schmidt

Program Manager

The AFOSR Program Manager currently assigned to the award

Gernot Pomrenke

Report Information - Annual Report

Reporting Period Start Date

06/15/2009

Reporting Period End Date

06/14/2013

Contents:

Abstract

Rolled-up microtube cavities were prepared for optical and electronic applications. For Optical components, the quality factor was greatly improved by introducing an axial confinement. Optical modes tuning was systematically investigated which led to a variety of optical sensing applications, including on-chip integrative microtube resonator for optofluidic sensing, dynamic molecular process sensing, and angular position detection of single nanoparticles. Add-drop configuration in microtube resonator was explored through microcavity-fiber coupling. A novel method for the fabrication of rolled-up diamond lattice photonic crystals was proposed. Finite element calculations support the proposed method. Optical spin-orbit coupling was realized in cone-like microtube cavity, which implies promising applications by manipulating photons in on-chip quantum devices. For electronic components, rolled-up capacitors were fabricated. Compacted metal-oxide field effect transistors withstanding ultra-small bending radii were prepared for integration into microfluidic application as electronic sensing devices.

Rolled-up photonics

1. Three dimensional confinement for optical resonances in rolled-up microtube cavities

1.1 Investigations and improvements on the optical quality of rolled-up SiO_2 resonators

Responsible scientist: Stefan Böttner
Reference: S. Böttner, et al. Opt. Lett. ***37****, 5136 (2012).*

The optical quality of resonators can be described by the quality (Q) factor where large numbers correspond to narrow resonant modes. A high Q factor is important in many applications. It is therefore of great importance to improve the Q factor of microtube cavities. By introducing a lobe-like structure onto the microtubes made of low refractive index material (SiO_2), three-dimensional confinement for optical resonances is realized. This kind of tube has many remarkable properties, such as weak optical absorption in visible spectral range, ultra smooth tube surface, and compact tube wall structure. As such, the Q-factor is extensively enhanced.

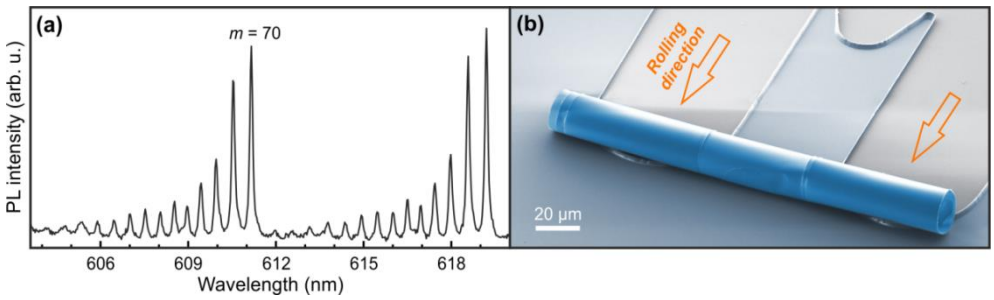

Figure 1. (a) Photoluminescence emission signal of a rolled-up resonator. The two fundamental mode peaks have a quality factor of 5400 and are followed by axial modes at shorter wavelengths. (b) Colored scanning electron microscope image of a rolled-up resonator.

The achieved Q factor in our resonators was found to be 5400 which is a huge improvement to the values reported in our previous annual reports. This result is important for all follow-up experiments as narrow optical modes are needed in most applications and experiments that exploit the optical confinement of light in rolled-up resonators.

1.2 Novel optical axial confinement in asymmetric microtube cavities

Responsible scientist: Libo Ma
Reference: V. Bolaños, et al. Opt. Lett. ***37****, 4284 (2012).*

We demonstrate a novel, flexible, axial confinement mechanism in asymmetric microtube cavity. Asymmetric cone-like microtube cavities were fabricated by unevenly rolling-up from pre-strained SiO/SiO_2 circular-shaped nanomembrane on sloped photoresist patterns. The high-Q modes are found only at the top region of the tube.

Figure 2(b) displays the PL spectrum of high-Q modes (top panel) with azimuthal modes M=35-37. Each set of these modes is fitted by a superposition of Lorentzian functions where three axial modes peaks are identified. The calculated peak positions (triangular marks) agree well with our experimental results. The high-order modes with spatially localized characteristics indicate an axial optical confinement in the tube cavity.

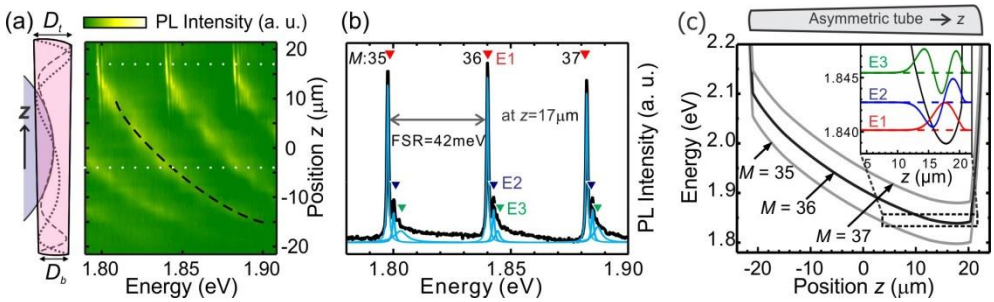

Figure 2. (a) Color-coded PL intensity map along the axis of an AMR. The left panel shows a sketch of the corresponding AMR cavity. (b) A high-Q mode spectrum with three high order axial modes in each azimuthal mode (M: 35-37) are shown. Their peak positions agree well with the employed theoretical model (triangular marks). (c) Calculated axial potential in the AMR for M = 35-37. The inset shows a magnified plot area with equal axial potential and z ranges. The potential minimum for M = 36 and the first three axial field distributions are depicted.

A photonic quasi-Schrödinger equation was employed to calculate axial potential well in the AMR cavity. The axial potential k_{ax} corresponding to each azimuthal mode considered in Fig. 2(b) is plotted in Fig. 2(c). In Fig. 2(c), the potential clearly shows a minimum located at the larger diameter side of the AMR. These results indicate that the tube diameter variation dominates the formation of axial potential well and the variation of refractive index is of minor importance. Moreover, the location of the axial potential well can be tuned along the tube axis by modifying the conical degree of the cone-like structure and/or the variation rate of effective refractive index of the tube wall.

2. Tuning of optical resonant modes in rolled-up microtube cavities

2.1 Tunable microtube resonators from shaped nanomembranes

Responsible scientist: Gaoshan Huang
Reference: G. S. Huang, et al. Appl. Phys. Lett. ***94****, 141901 (2009).*

Tunable microtube resonators have been fabricated by releasing pre-stressed circular SiO/SiO_2 nanomembranes, where the rotations vary with the distance away from the middle of the tube (see the optical microscope image of an ordered microtube array in the inset of Fig. 3.). The photoluminescence (PL) spectra from these microtubes exhibit modulations in intensity. Finite-difference time-domain (FDTD) simulation reveals that the modulation is caused by optical resonant modes from light circulating and interfering in the tube wall.

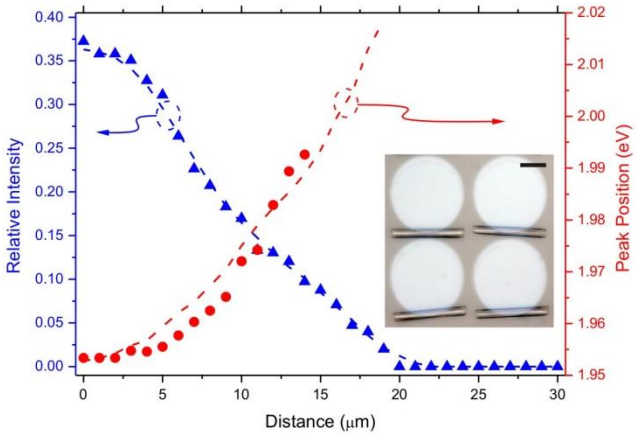

Figure 3. Blue triangles show the relative intensity of a mode (azimuthal number *M*=29) as a function of the distance from the middle of the tube. The blue dashed line is a guide to the eye. The red circles display the experimental result of peak position (*M*=29) as a function of distance. The result from

FDTD simulation is given as red dashed line. The inset shows an optical microscope image of an ordered microtube array formed on circular patterns (scale bar: 20 μm).

A series of PL spectra were measured along the microtube axis, and the evolution of the relative intensity of a resonant mode (~1.95 eV; *M*=30) is displayed in the blue triangles. The relative intensity reaches a maximal value at the middle of the microtube with maximum rotations. Whereas, at the regions near the ends of the microtube, the thinner tube wall weakens the light confinement and the resonant modes can no longer be observed. In addition to the evolution of the relative intensity, the structure of the microtube has significant influence on the mode positions. The resonant modes shift continuously to higher energy when moving from the middle to the end of the microtube (red circles). To understand this shift qualitatively, we can consider the cross section of a microtube as a circular waveguide. The decrease of the rotations/tube wall thickness shortens the path of the light circulating around the circle, leading to a decrease of the effective refractive index. As a consequence, the modes should move to shorter wavelength/higher energy. The shift quantitatively calculated by FDTD simulation (red dashed lines) fits the experiment result very well.

2.2 Spectral tunability of rolled-up microtube resonators on glass

Responsible scientist:Vladimir Bolaños
Reference: V. A. Bolaños, et al. Opt. Lett. ***34****, 2345 (2009).*

Microtubular resonators fabricated by the release and roll-up of strained nanomembranes guide light along the tube wall in the azimuthal direction. The evanescent field of the resonant modes interacts with the media surrounding the micro-resonator, suggesting potential applications for on-chip components like filters and sensors. In order to fine tune the resonant modes, a stepwise study of a one-by-one monolayer (ML) of Al_2O_3 coating on a SiO/SiO_2 rolled-up microtube with atomic layer deposition is carried out. As shown in Fig. 4(a), rolled-up microtubes are fabricated on a transparent glass substrate, and a scanning electron microscopy (SEM) image of the tube array is presented in Fig. 4(b). By ALD coating, a controllable red shift of Transverse Magnetic (TM) polarized resonant modes (labelled by solid circles and empty triangles in Fig. 4(c) measured by PL is obtained over a wide spectral range. The measurements is well reproduced by FDTD simulations. In addition, a new group of resonant modes emerge when the Al_2O_3 coating is thicker than 200 ML (~ 20 nm). These modes are Transverse Electric (TE) polarized (labelled by solid triangles) perpendicular to the previous group. Therefore, as the wall thickness increases, the diffraction loss of the TE modes decreases, allowing the microresonator to simultaneously support both TM and TE resonant modes. FDTD simulations reveal a progressive increase of the microtube refractive index after the consecutive Al_2O_3 coating, which cause a higher contrast between the microtube and the surrounding media resulting in the observed mode shifts.

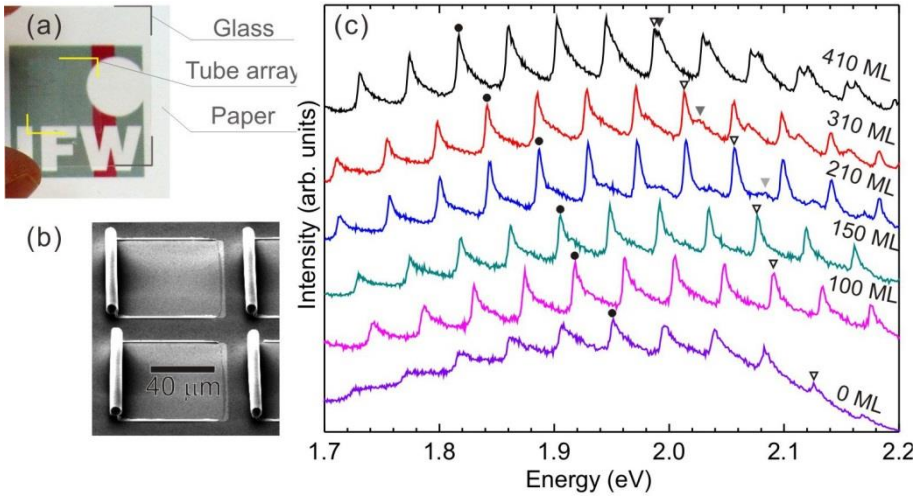

Figure 4. (a) Rolled-up microtubular cavity array fabricated on a transparent glass substrate; (b) SEM image of microtubes rolled up from a square pattern. (c) Photoluminescence (PL) spectra of a ~7 µm diameter tube after coating with Al_2O_3 layers with increasing thicknesses (in MLs). Symbols mark the evolution of two TM modes (solid circles and empty triangles) and one TE mode (solid triangles).

2.3 Tuning of optical resonances by asymmetric modification of microtube cavities
Responsible scientist: Libo Ma
Reference: L. Ma, et al. Opt. Lett. ***36****, 3840 (2011).*

Rolled-up microtubes can be used as wavelength tunable emitters by deliberately introducing asymmetry into the structure. In this work, optical resonances are tuned by stepwise deposition of SiO_2 onto the rolled-up tube cavities. During the deposition, a SiO_2 nano-cap is grown on the top side of the microtubes which are fully integrated on the substrate. In this way the microtube cavities are asymmetrically modified.

Two kinds of microtubes are prepared for the resonance tuning, relatively flexible tube-I and relatively rigid tube-II. The asymmetric modifications of the microtube cavities are schematically shown in Fig. 5(a) and b for tube-I and tube-II, respectively. Every mode in the spectrum is labelled with the corresponding azimuthal mode number *M*, as shown in Fig. 5(c). Spectral blueshifts followed by redshifts of the resonant modes are observed in tube-I. During the post-deposition process, the competition between better confinement and enhanced light losses is responsible for the evolution of the Q factor. Figure 1-d shows the PL spectrum of tube-II with an FSR of around 17 nm. Contrary to tube-I, exclusively redshifts of the resonant modes are observed after SiO_2-deposition in tube-II. Moreover, transverse-electric (TE) modes emerge along with resonant TM mode peaks due to the thicker tube wall in tube-II.

Calculations of modulated optical resonances are performed by using a two-dimensional ring resonator model and perturbation theory. Based on the calculations, the post-deposited SiO_2 nano-cap results in mode redshift and an oval-shape deformation in flexible tube cavity induced by SiO_2 deposition leads to blueshift. In Fig. 5(e) and (f), we select mode $M = 39$ for tube-I and $M = 31$ for tube-II as examples to show the two kind of tuning mechanisms. The competition between shape deformation and effective increase of the tube wall thickness results in blueshifts followed by redshifts of the resonant mode in tube-I. In this case, a shape deformation $D = 36.2$ nm of the cavity structure is estimated. Since tube-II is robust enough to prevent any shape-deformation during SiO_2 deposition, only redshift of resonant modes can be observed during post-depositions.

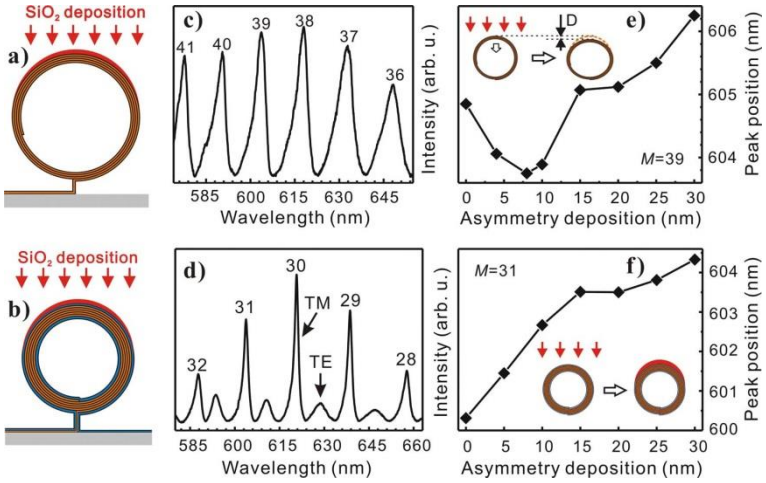

Figure 5. Sketch of tube cross-section during SiO_2 deposition for tube I (a) and tube-II (b). TM resonant modes are labelled with the calculated azimuthal mode number M for tube-I (c) and tube-II (d). TE modes emerge along with resonant TM in tube-II. e) Mode shift for M = 39 in tube-I as a function of the thickness of post-deposited SiO_2. The inset shows the definition of shape deformation D. f) Mode shift for M = 31 in tube-II. The inset shows a sketch of post-deposited SiO_2 nano-cap on tube cavity.

The wavelength-dependent resonance tuning opens a way to simultaneously tune different modes in one optical microtube cavity. Furthermore, the high optical sensitivity for small perturbations on the microcavity offers a possible implementation of an efficient sensing function of the microtube resonators.

2.4 Dynamic axial mode tuning in a rolled-up optical microcavity

Responsible Scientist: Shilong Li

Reference: S. Li, et al. Appl. Phys. Lett. ***101****, 231106 (2012).*

Dynamic axial mode tuning is demonstrated by means of near-field probe in a rolled-up optical microcavity. In this study, the microtube cavities were rolled-up from U-shaped patterns. An axial confinement is formed in the lobe region.

The probe was introduced, and scanned along the axial axis of the microcavity as illustrated in Fig. 6(a). The first 5 axial modes should be located within the lobe and have electric field distributions that vary with lateral position as shown in Fig. 6(c). By measuring the micro-photoluminescence (μ-PL) spectra from the microcavity with and without the probe present in the middle of the lobe, the redshift for each of the axial modes was measured. In excellent agreement with the axial confinement model and perturbation theory used, an alternating pattern of shifting is observed due to alternating magnitudes of field-probe overlap as shown in the upper part of Fig. 6(b). The fundamental mode, which has the most extensive overlap when the probe is in the middle of the structure, shifts the most, while the second mode shifts very little due to the central node present. The third mode experiences a pronounced shift again.

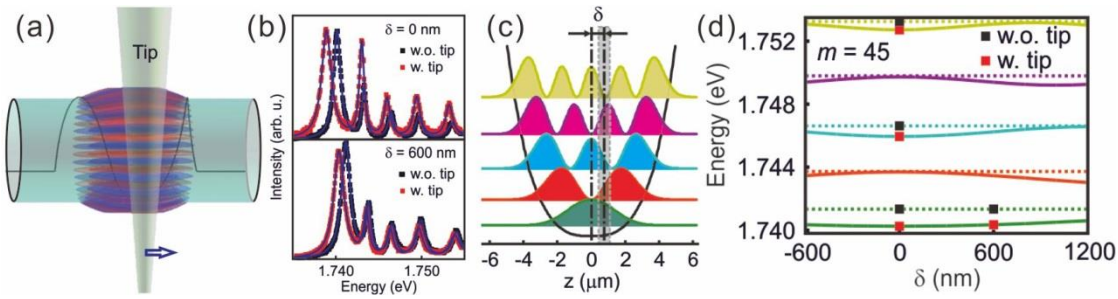

Figure. 6. (a) Schematic of the lateral probing process. The electric field plotted corresponds to m = 45 azimuthal and fundamental axial mode. (b) Measured details of the m = 45 azimuthal mode with and without the probe at two lateral positions separated by 600 nm. (c) Calculated axial confinement profile, showing the first five axial modes as a function of lateral position, z. The predicted alternating overlap of the mode energies with the probe is confirmed in our measurement. (d) Predicted axial mode shift as a function of lateral position. Dashed lines indicate the predicted mode position in the absence of the probe. Solid lines indicate the calculated mode position in the presence of the probe. Solid squares are the experimental peak positions for the data shown in (b).

In contrast to the tuning demonstrated here, the same effect could be used for lateral position detection. Based on an initial PL measurement of the microcavity modes, the relative peak shifts for a field perturbing analyte such as a nanoparticle could be calculated as a function of lateral position and size. In future experiments, particle detection with lateral position resolution would be enabled by the relative peak positions of the axial modes.

3. Rolled-up microtube cavities for optical sensing

3.1 Enhanced liquid sensing of rolled-up microcavities with subwavelength wall thicknesses
Responsible Scientist: Gaoshan Huang
Reference: G. S. Huang, *et al*. ACS Nano **4**, 3123 (2010).

In optical ring resonators, the whispering gallery modes form due to total internal reflection of light at the boundary between the high and low refractive index media. The evanescent field penetrates into the low refractive index medium and interacts with the materials near the interface, leading to a wavelength shift of the light circulating in the optical ring resonator. Thus, sensing applications of ring resonators are realized by simply detecting spectral shifts of the optical resonant modes. In this work, we fabricated optical microcavities with defined diameters and subwavelength wall thicknesses.

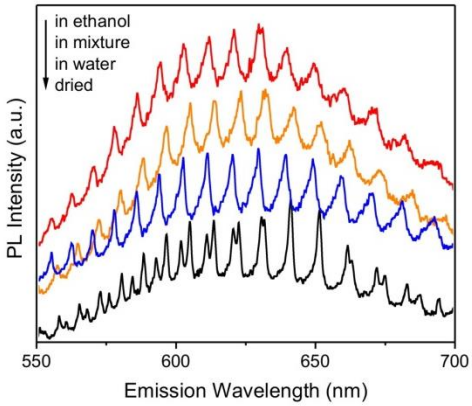

Figure 7. PL spectra of an optical microtube cavity with a diameter of ~9 μm in air, de-ionized water, ethanol, and water/ethanol mixture (1:1 in volume). All microtubes were excited by a frequency doubled Nd-YVO4 laser operated at 532 nm. The intensity of each spectrum is normalized to its strongest mode.

Whispering gallery modes are observed from SiO/SiO_2 rolled-up microcavities and their spectral peak positions shift significantly when measurements are carried out in different surrounding media (see Fig. 7). Spectral analyses reveal that modes shift to longer wavelength with increasing the refractive index of the surrounding medium, thus indicating excellent sensing functionality of these microcavities. A maximum sensitivity of 425 nm/refractive index unit can be achieved for the SiO/SiO_2 microtube ring resonators. This is caused by the pronounced propagation of the evanescent field in the surrounding media due to the subwavelength wall thickness design of the microcavity, and is much higher than previous results obtained from glass capillaries. Analytical calculations as well as FDTD simulations are performed to investigate the light confinement in the optical microcavities numerically, and the results describe the experimental mode shifts very well. We expect that this kind of rolled-up optical sensor can be easily integrated into a bio-analytic tubular microchannel for

lab-on-a-chip applications. For instance, a multifunctional lab-in-a-tube may be fabricated in this way to detect and analyze individual cells, biomolecules, and their bioactivities.

3.2 Three-dimensional confinement in asymmetric microtube cavity for optofluidic detection
Responsible Scientist: Libo Ma
Reference: L. Ma, et al. Appl. Phys. Lett. ***101****, 151107 (2012).*

The efficient axial confinement in asymmetric tube facilitates their application such as optofluidic detections. For optofluidic detection, the tube was filled with aqueous salt solution (0.65 mg/l). The presence of the new medium inside the microtubes causes spectral shifts of the resonant modes. The lower PL spectrum shown in Fig. 8(a) corresponds to the measurement of an initially empty microtube resonator in air. In this tube, up to eight axial resonant modes are resolved for some azimuthal modes due to the deep and narrow axial potential well. After inserting the salt solution, the axial multi-modes are still present but appear on the high energy side of azimuthal modes with larger M due to a stronger confinement caused by the liquid core. The calculated mode positions of the first axial resonant modes for M = 39-42 are marked (triangular marks). Figure 8(b) shows the average mode spacing for each group of axial modes M. It is found that the axial mode spacing increases when the tube is filled with salt solution, which is caused by a deeper axial potential well due to the presence of salt solution core. Here we proposed a detection methodology using axial mode spacing changes detected from the rolled-up resonators. By observing and measuring the axial mode spacings corresponding to a particular azithumal mode M, the refractive index of the fluid in the core can be extracted by comparing the mode spacings against a known reference. This sensing ability could be an alternative/complement to the traditional method of monitoring the spectral azimuthal mode shifts.

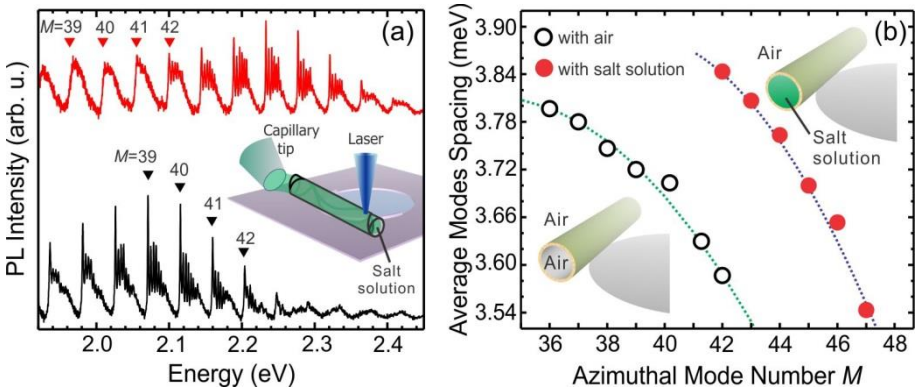

Figure 8. (a) Background-subtracted PL spectra of an empty microtube (lower spectrum) and a tube filled with aqueous salt solution (upper spectrum). The azimuthal mode numbers as well as the calculated mode positions of the first axial resonances are indicated for M = 39-42. The inset shows the sketch of liquid core filling for optofluidic detection. (b) Average axial mode spacings for empty tube (empty circles) and solution-filled tube (red circles) as a function of the azimuthal mode number M. The dotted lines are guides to the eyes. The bottom left inset shows the sketch of the empty rolled-up tube while the upper right inset shows the case of the tube filled with salt solution.

The ability to detect fluids in the hollow core of micrometer sized tubes is well-suited to fabricate liquid-channel sensors for picoliter volumes of diverse analytes; or, vice versa, to determine the refractive indices of liquids by monitoring the mode positions. These results, along with the AMR tubes facile on-chip fabrication, facilitate their application in more complex devices that could exploit their conical shape; for example optofluidics, lasing or bio inspired sensing/detection by confining a biological component.

3.3 Lab-in-a-Tube: on-chip integration of glass optofluidic ring resonators for label-free sensing applications
Responsible scientist: Stefan Harazim
Reference: S. M. Harazim, et al. Lab Chip 12, 2649 (2012).

A fully operational on-chip refractrometric sensor system for label-free sensing applications was performed. The key component of the system is an optical active and transparent glass (SiO_2) microtube fabricated by using rolled-up nanotech on polymers. The sensing mechanism of the so called rolled-up optofluidic ring resonator (RU-OFRR) relies on the response of the whispering gallery modes (WGM). An installed viewport on each microtube enables the exact aligned excitation and monitoring of WGM modes with a PL detection system under constant ambient conditions while exchanging the content of the RU-OFRR with liquids of different refractive indices. The improved sensor capabilities were investigated regarding signal stability, sensitivity and reliability. The sensitivity, the response of the WGM to the change of the refractive index of the liquid, of the integrated RU-OFRR is reported to values of up to 880 nm/RIU.

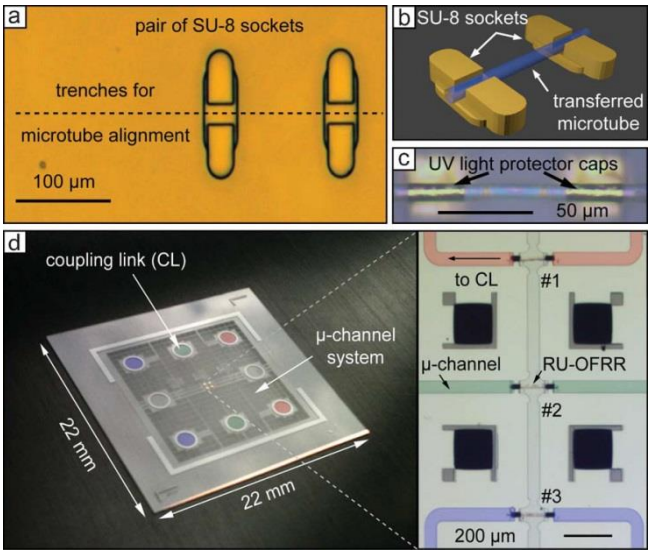

Figure 9. Transfer, protection and integration of a microtube. (a) Optical image of a pair of SU-8 10 sockets for elevating a transferred RU-OFRR. The dashed line indicates the position of the trenches in the sockets used as alignment guides during the transfer. (b) 3D sketch of a transferred microtube placed into the socket structures. (c) Optical image of a transferred microtube with applied UV-light protector caps on top. (d) Overview of the entire chip with a microchannel system and the coupling links. The zoomed-in view depicts three labeled rolled-up OFRRs integrated into a microchannel structure. The colored channels are connected to the corresponding coupling links on the chip structure with the same color.

The dashed line in the optical image in Fig. 9(a) indicates the trench in the sockets where the transferred microtube will be placed, as depicted in the sketch in Fig. 9(b). The location, orientation and number of sockets can be chosen on demand, depending on the intended application and size of the microtubes. To avoid polymerization of the SU-8 photoresist inside the microtubes during the structuring of the microchannel system, protector caps were deposited onto the microtube. The microfluidic system is formed by a photo-lithographically patterned SU-8 10 polymer layer with a height of 20 mm. The photograph in Fig. 9(d) shows the target microchip substrate containing the sensors, defined structures such as the coupling links (CL) for the in- and outlets of the system and a microchannel system.

The process of the device fabrication is reproducible, reliable and shows long term signal stability. Further studies focus on the fabrication on the integration of sensors able to perform specific label-free detection of molecules. Furthermore the integration together with other tubular sensors based on electric or magnetic principles are planned to be realized.

3.4 Self-assembled microtubular opto-chemical sensors for dynamic molecular process detection
Responsible scientist: Libo Ma
Reference: L. Ma. et al. Adv. Mater. 25, 2357, (2013).

The asymmetric microtube cavity is used as an opto-chemical sensor for dynamic molecular process detection. The tube surface is covered by a 30 nm thick film of hafnium oxide (HfO_2), which is introduced for molecular adsorptions. Due to the subwavelength thick tube wall, the evanescent field substantially leaks out of the tube surface, greatly enhancing the surface detection sensitivity. When the surface environment slightly changes, the evanescent field is perturbed and the resonant modes either red- or blue-shift. By monitoring the mode shift in real time, the dynamic molecular process is detected by the microcavity.

Perturbation theory is used to calculate the mode shift induced by molecular adsorption/desorption on the cavity surface. As expected, the higher refractive index molecule layer will lead to a larger mode shift, as shown in Fig. 10(a). In this tube cavity, sub-monolayer of H_2O and C_2H_5OH can be easily detected. Figure 10 (c) shows the detection of the dehydration effect on the nanomembrane surface. The tube surface was initially wetted with ~ 7.3 monolayers of H_2O. After the dehydration by ethanol, only ~1 monolayer of H_2O was removed. The suppression of the ethanol dehydration effect suggests that the H_2O molecules assemble into a durable ice-like layer on the surface. In contrast to previous reports, here the robust ice-like H_2O molecule structure was detected at room temperature on a nanomembrane platform assisted by optical resonances.

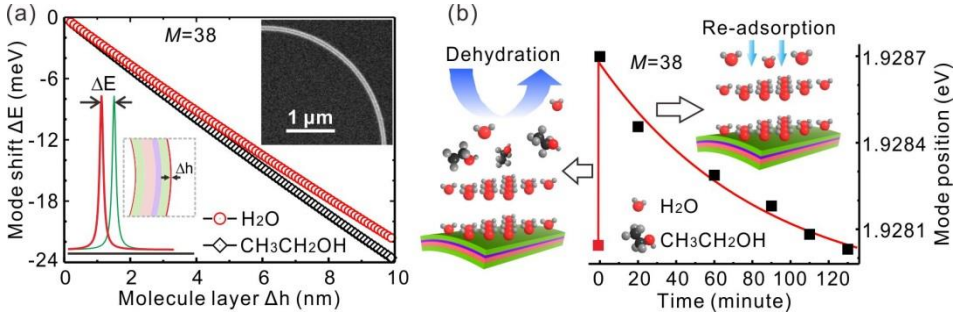

Figure 10. (a) Optical resonant mode (M=38) shift (ΔE) induced by adsorbed molecule layer (Δh) on both outer and inner tube surfaces calculated using perturbation theory for H_2O and C_2H_5OH molecules, respectively. The upper right inset shows the cross-section SEM image of the part tube wall rolled-up from nanomembrane. The bottom left inset shows the schematic of resonant mode shift in response to adsorbed molecular layer on the nanomembrane surfaces. (b) Mode (M=38) blueshift of ΔE = 0.66 meV implying desorption of around one H_2O monolayer after ethanol dehydration on the tube surface. The subsequent redshift of the mode position indicates a re-adsorption process of the H_2O molecules which is fitted by the LDF model.

The ability of our microtube cavity to probe molecular level changes on the sensing surface constitutes a versatile platform for the detection of diverse surface phenomena in a label-free fashion.

3.5 Angular position detection of single nanoparticles on rolled-up optical microcavities

Responsible scientist: Shilong Li

Reference: S. Li, et al. Phys. Rev. A 88, 033833, (2013).

Nanoparticle position detection is prevented in highly symmetric whispering gallery mode optical microcavities due to the redistributable electric field of resonant light therein. In asymmetric tubular microcavities, the optical resonant modes are split and locked to the spiral-shaped geometry. The discriminative responses of neighboring resonant modes to a local disturbance provide a method for angular position detection of a single nanoparticle on a rolled-up optical microcavity. These findings add new functionality to microcavity applications and a deeper understanding of cavity electrodynamics.

The modes split differently depending on the nanoparticle's angular position, which is defined as the number of degrees the nanoparticle is away from the outer step in the counter-clockwise direction (see Fig. 11(a)). Figure 11(b) shows the m = 17 mode in the absence of

the nanoparticle and at two different angular positions. In a rolled-up microcavity, however, the single nanoparticle will modify the intrinsically split modes as a function of the angular position. Figure 11(c) shows how the splitting of the m = 17 mode varies as a function of angular position along the rolled-up microcavity. The evolution of each split mode exhibits periodic behaviour. Due to the periodicity of the distribution, the nanoparticle will perturb the mode in a periodic way leading to an angular spatial frequency equal to the number of antinodes. By monitoring the resonant energies of three modes together, the spectroscopic detection of the angular position of a single nanoparticle on a rolled-up optical microcavity is demonstrated. Based on this strategy, the functionality of optical microcavities as a detector is greatly enhanced.

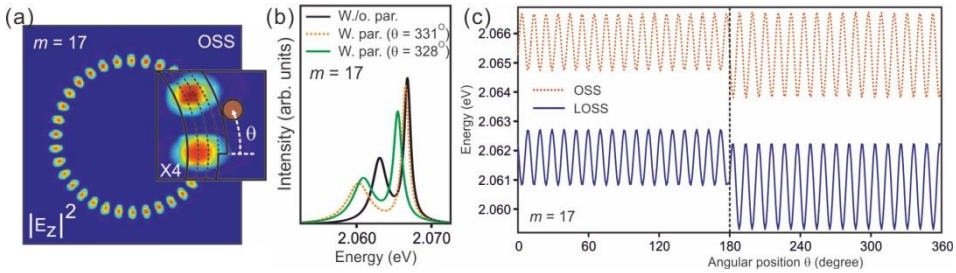

Figure 11. (a) Electric field profile of the OSS mode for m = 17. The location of a nanoparticle is defined by the azimuthal angle θ counter-clockwise from the outside step. (b) Spectra for m = 17 in the absence of the nanoparticle, and with the nanoparticle at two different angular positions. (c) Resonant energies of the LOSS and the OSS modes as a function of the nanoparticle position.

4. Microtube-fiber coupling

4.1 Optical filter of ring-waveguide

Responsible scientist: Elliot Smith

Much work has been done on filters using ring resonators to filter out certain wavelengths and much interest has been shown in their integration capabilities. By placing a ring resonator next to a waveguide, light can be leaked out of the guide into the resonator leading to a drop in signal at the detector for a particular wavelength(s). We have proposed using our rolled-up technology to act as a drop filter for waveguides. By placing a SiO_x tube on top of an SU8 waveguide, we hope to achieve a filtering of through-put light in accordance to the modes (wavelengths) which are picked up and resonate within the tube.

Work has been done by our group with respect of the WG modes we can resonate within our tubes, which has allowed us to move forward by developing SU8 waveguides on top of silicon wafers to be used as our signal waveguide to demonstrate such a filter. We have developed a reproducible method for creating SU8 waveguides and have demonstrated their ability to guide light in a number of structures, Fig 12(a) and (c). We have precise placement of our waveguides Fig. 12(a).i and have preliminary work on placing our previously designed SiOx tubes on top of our guides. One can see in Fig 12(a).iii an increased intensity in the SiOx tube where it makes contact with the SU8 waveguide. We have also explored using our rolled-up tubes to transfer information from one guide into another, for instance in crossing waveguides. We have done preliminary theoretical, Fig 3b, and experimental, Fig. 12(c), work to realize such a device. The next step is to study the effects of placing our tubes on top of the cross section of the two guides to study the effects of increased or redirection of the transmission of light.

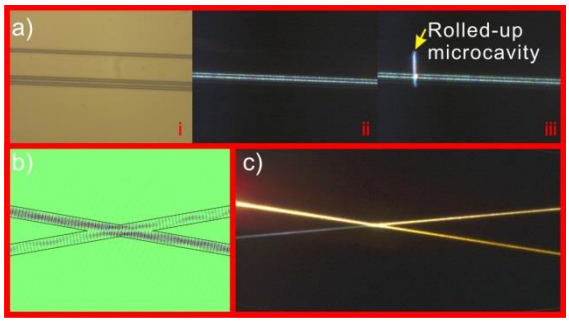

Figure 12. The experimental steps made so far to realizing our proposed optical filters using rolled-up technology3. a) i) Three 5x4µm SU8 waveguides are separated by 5 and 45µm (from the center guide) are shown under normal illumination. ii) shows the middle guide being illuminated from one end by a white light laser and iii) illustrates our ability to precisely place a rolled-up SiOx tube (~5µm diameter) on top of the guides. Early work has been done in using the Rolled-up tubes as drop filters in crossed waveguides. Currently work has been performed to understanding the effects of crossed waveguides without a tube on top through b) simulations and c) experimental results using SU8 waveguides fabricated on silicon substrates.

4.2 Fiber interfaced rolled-up resonators in add drop configuration

Responsible scientist: Stefan Böttner
Reference: S. Böttner, et al. Appl. Phys. Lett. 102, 251119 (2013).

Many optical studies on rolled-up resonators are based on embedded emitters in the resonator walls excited and detected by a photoluminescence (PL) detection system. Emission of the emitters is mainly observed in the visible spectral range at around 600 nm so that experiments are limited to this range. Normally, many supported optical modes are excited at the same time making detailed studies on selected modes difficult. Additionally, the free space laser beam used for excitation is cumbersome and complicates integration and shielding of the resonator from the outside world.

To avoid these problems a new experiment based on tapered fibers was designed to explore new light coupling methods based on evanescent waves. To achieve this coupling, fibers need to be tapered to diameters of about 1-3 µm and brought close to a rolled-up resonator, light can then couple to the resonator and excite resonant modes. Now experiments can be performed with light at any wavelength guided by the fiber and the fibers can in principle be integrated in a packaged chip. Especially interesting is the telecommunication wavelength range at around 1550 nm because it is also common in the field of silicon photonics where waveguides are used.

The developed fiber setup and a rolled-up resonator interfaced with a tapered fiber is shown in Fig. 13(a) and (b). During the measurement the wavelength of a laser is scanned in the telecom wavelength band and the transmission through the coupled fiber is detected by a photodetector. Resonances appear as dips in the spectrum as opposed to peaks in PL measurements. Therefore the rolled-up resonator can serve as a filter element in photonic networks where it could be tuned by changing the surrounding media as shown in microfluidic sensing experiments.

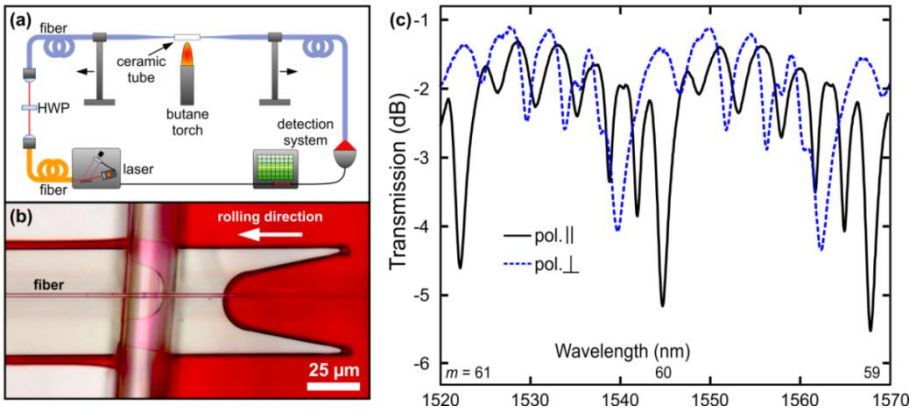

Figure 13. (a) Schematic drawing of the fiber tapering setup also used for coupling experiments. Transmission through fiber is monitored by detection system while laser is tuned from 1520 nm to 1570 nm. Polarization of light in fiber is controlled by half wave plate (HWP). (b) Focus stacked micrograph of rolled-up resonator coupled to tapered fiber. (c) Normalized fiber transmission signals while coupled to a rolled-up resonator for two orthogonal fiber input polarization states.

Since our resonators demonstrated capabilities for the use as filter components we extended this application and developed a vertically aligned rolled-up add-drop filter [see Fig. 14]. In this work a resonator was sandwiched between two tapered fibers. The laser source was connected to the input of one fiber and the output of both fibers was monitored. For every resonance dip in the transmission fiber, a peak in the second (drop) fiber is visible. Light is therefore vertically transferred from one fiber to another making this device highly interesting for future stacked optical chips where signals need to be transferred in the vertical direction.

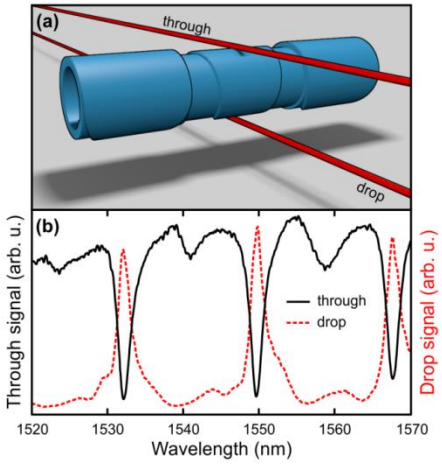

Figure 14. (a) Schematic image of a lifted resonator sandwiched between two tapered fibers (red). (b) Transmission spectrum of through fiber (black solid line) and drop fiber (red dashed line).

5. Rolled photonic crystal

Responsible scientist: Matthew Jorgensen
Reference: M. R. Jorgensen, et al. Phys. Rev. A 87, 041803 (2013).

A novel method for the fabrication of full band gap photonic crystals was proposed by rolling pre-patterned pre-strained membranes into three dimensional tubular structures. This fabrication method raises interesting questions regarding the limits of currently used photonic crystal theories, which assume a linear and infinite lattice. A two dimensional model of the rolled-up photonic crystal was studied using finite element analysis. It was found that, within the context of our structure, certain limits to the size and radius of curvature could be identified. These findings aid in the future fabrication of rolled-up photonic crystals and provide insight into the limits of photonic crystal theory.

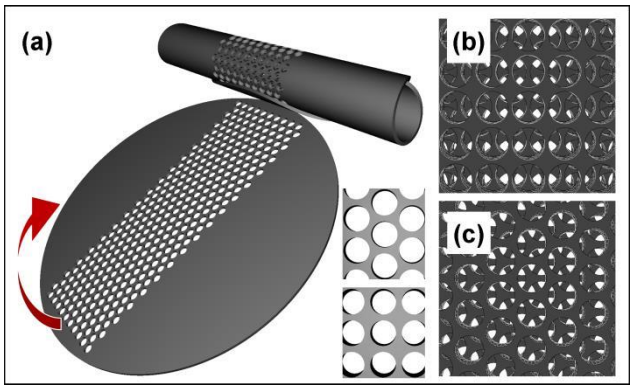

Figure 15. Schematic of the proposed method for fabricating three-dimensional photonic crystals by rolling pre-strained pre-patterned membranes. (a) The lattice of holes overlaps with itself as it rolls. (b) If rolled from a triangular lattice, a <111> diamond structure, similar to Yablonovite, can be formed. (c) If rolled from a square lattice, a <100> diamond structure possessing a full band gap can be formed.

Work towards the fabrication and theoretical analysis of novel diamond-based photonic crystals (PCs) began during the last part of the award period. Due to the difficulties associated with the fabrication of full band gap PCs which operate at visible wavelengths, we proposed a scheme to combine two-dimensional nanofabrication technology and rolled-up nanotech technology to construct a rolled-up diamond based PC. Under this scheme, pre-strained titania membranes on sacrificial layers would be patterned with a two-dimensional lattice of holes using EBL patterning and dry etching techniques. Following patterning, the sacrificial layer would be removed allowing the membrane to roll into a cylindrically shaped three-dimensional PC.

The proposed fabrication method immediately raises interesting fundamental questions regarding how standard PC theories, which assume an infinite lattice satisfying Bloch conditions, relate to real PCs which are finite and might not satisfy Bloch conditions. To address these questions, and to gain insight required for fabrication of a rolled-up PC, finite sized and bent PCs were modeled and studied using finite element analysis.

It was found that there are identifiable limits to the number of periods and amount of distortion which a PC can tolerate and still maintain its band gaps. In one segment of the theoretical work, it was found that a minimum of 6 periods are required to effectively inhibit light inside a PC within the band gap frequencies. In another segment of the work, it was found that in a two-dimensional representation of a rolled-up PC the band gaps are remarkably resilient to bending distortions. Inhibition of light within the band gaps was maintained up to bending radii of just 20 lattice units.

An extensive study of the different diamond lattices available by rolling square and triangular two-dimensional lattices was also completed using more conventional Bloch-iterative methods. Interestingly, it was found that the robust Yablonovite diamond structure could not produce a full band under our conditions and available refractive index (up to approximately 2.9). However, a full band gap is accessible by rolling a square lattice of holes if the refractive index is above 2.3.

Preliminary experimental work has commenced. Rolled-up titania membranes having the required thickness, refractive index, and number of windings have been fabricated. Separately, work has progressed towards the patterning of the membranes using a variety of methods.

6. Optical spin-orbit coupling in cone-like microtube cavities

Responsible scientist: Libo Ma

Photons circulating around a tilted closed trajectory in cone-like microcavities experience a spin-orbit coupling. The resultant geometric phase together with the basis vectors conversion leads to a polarization change from linear to elliptical polarization, performing a non-cyclic non-Abelian evolution.

Experimentally, cone-like tubular microcavities are prepared by rolling-up pre-strained nanomembranes. This kind of tube exhibits a weakly anisotropic inhomogeneous refractive index due to the tubular curvature and the variation of wall thickness. The experiments were performed using a micro-photoluminescence setup. A laser beam (Nd:YAG laser line at 532 nm) was focused on the larger tube side where high-quality optical modes can be excited. The polarization states and orientations were measured by rotating a half-wave-plate in combination with a polarizer in front of the detector.

When the light propagates in the thin-walled microtube, the electric field vector rotates around the tube axis due to the cone-shape of the microtube. This rotation generates an effective magnetic field (L) along the tube axis, which plays a role of the orbital angular momentum. The right and left circular polarization basis states carry spin angular momenta with opposite signs. Due to the spin-orbit coupling, the right and left circular components acquire a geometric phase with opposite signs together with a conversion between the two basis vectors. This process is experimentally revealed by the resultant elliptical polarization with the major axis tilted away from the tube axis. The tilt angle reflects the occurrence of geometric phase while the ellipticity indicates the vectors conversion.

The conversion of amplitude from one circular component to the other leads to an increasing degree of elliptical polarization during the evolution. The occurrence of geometric phase and mode conversion causes the polarization state to evolve along a spherical spiral approaching the circular pole on a Poincaré sphere, thus manifesting the behaviour of non-cyclic geometric phase. In this process the two circular coefficients vary in an opposite way and result in the vector splitting of the spinning photons in a Hilbert space. This can be viewed as an analogy to the spin-Hall effect of light in a Hilbert space.

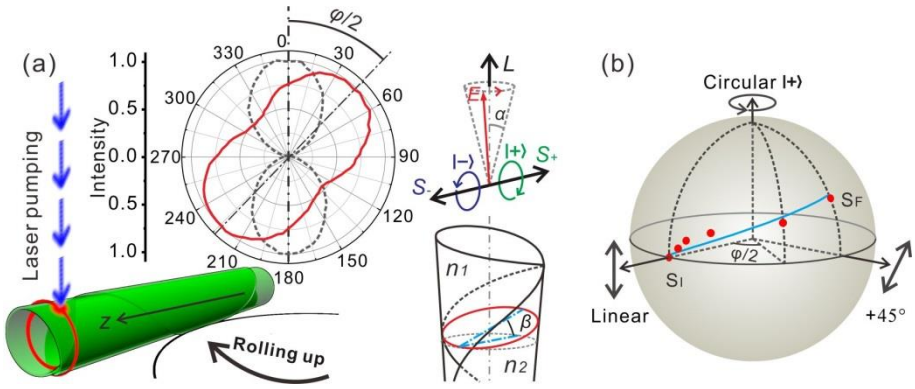

Figure 16. Photons change from linear to elliptical polarization state due to the spin-orbit coupling in a cone-like microtube cavity. (a) A cone-like tubular microcavity rolled up from a circular patterned nanomembrane is measured by a laser confocal microscope. Linearly polarized light turns to elliptically polarized with the major axis tilted out of the tube axis, as shown in the inset. (b) An effective magnetic field L is generated in the cone-shaped tube, allowing for an interaction with the spin angular momentum. (c) A series of polarization states (red dots) are plotted on a Poincaré sphere. The trace (blue solid line) shows a non-cyclic evolution from the linear polarization state to those with the elliptical polarization.

This work is interesting for fundamental studies and implies promising applications by manipulating photons in on-chip quantum devices, in particular, for quantum information technologies.

Rolled-up Nanoelectronics

1. Energy storage elements based on hybrid organic/inorganic nanomembranes

Responsible Scientist: Carlos César Bof Bufon
Reference: C. C. Bof Bufon, et al. Nano Lett. 10, 2506 (2010).

We demonstrate that self-assembly methods combined with standard top-down approaches are suitable for fabricating three-dimensional ultra-compact hybrid organic/inorganic electronic devices, such as self-wound capacitors (UCCaps), manufactured in parallel on a single chip (Fig. 17a). In addition to reducing the device footprint by the rolling process, the bottom metallic plate (red strip in Fig. 17a-b) mechanically touches the top oxide layer so that the final active capacitor area increases. For a large number of rotations (N), this effect is equivalent to connecting two unrolled capacitors in parallel.

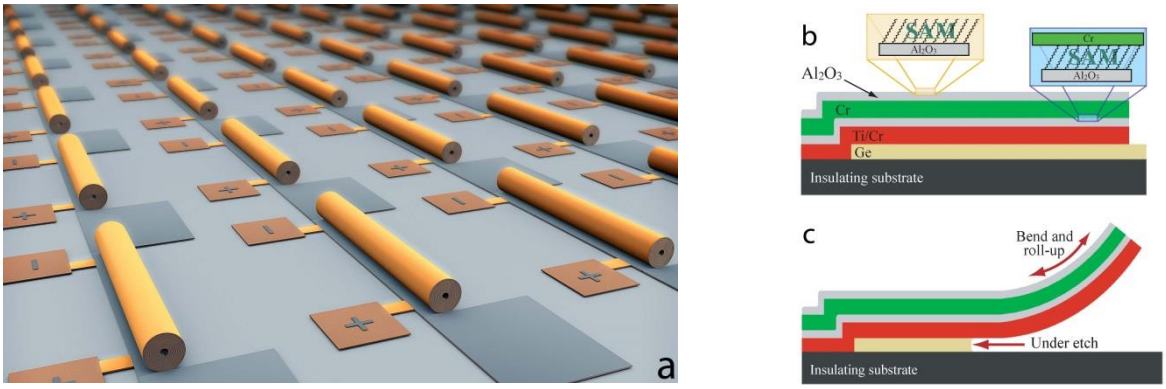

Figure 17. (a) Illustration of a parallel array of ultra-compact energy storage elements: (b) Deposition of the multi-stack layer. (c) The selective etching of the sacrificial layer releases the hybrid nanomembrane to form the roll-up device.

In addition of using pure Al_2O_3 as the dielectric layer, we also create a novel variety of energy storage elements by embedding high-k oxides layers (HfO_2 and TiO_2) into the Al_2O_3 matrix. The increasing of the capacitance per footprint was obtained when incorporate HfO_2 and TiO_2 into a rolled up devices. In order to keep the leakage current under acceptable levels ($< 10^{-3}$ A/cm^2 at 1V), HfO_2 and TiO_2 are placed in between the Al_2O_3 layer.

Due to the synthetic tailorability of organic molecular systems, their incorporation in inorganic elements gives rise to novel devices with almost limitless chemical and biological functionalities. To demonstrate this advantage, we have self-assembled phosphonic acid anchor groups (SAM) into the inorganic capacitor structure. The integration of organic molecules provides further free parameters to tune the properties and extend the range of applications of the final self-wound device.

2. High performance nanomembrane field-effect transistors with ultra-small bending radii for compact three-dimensional microfluidic integration

Responsible scientist: Daniel Grimm
Reference: D. Grimm, et al. Nano Lett. 13, 213, (2013).

The fabrication of flexible electronic devices has attracted broad interest to create new three-dimensional electronics such as wrapable solar cells, pressure sensors and paper displays. The adaption to uneven surfaces or repeated tight bending upon crumpling requires high mechanical flexibility of the circuits. Typically, the active semiconducting channels consist of organic material and recently, thin films of otherwise rigid semiconductors such as GaAs, Si and SiGe were successfully employed. The critical minimum bending radius of the flexible electronic devices is limited by the mechanical strain-induced damage deteriorating their performance. This radius is normally found in the millimeter scale, mainly depending on the overall thickness of the free-standing device. By scaling down the thickness of the flexible substrate support, organic transistors working with bending radii

down to 0.1mm could be demonstrated. Here, we introduce a new fabrication route of free-standing inorganic thin film transistors with ultra-small bending radii of less than 5µm (Fig. 18). The rolled-up field effect transistors exhibit high electronic performance such as On-Off ratios of more than 100,000 and Gate swings of around 160mV/dec (Fig. 18c). The thin film transistors are driven in the depletion mode where the gate potential acts directly on the thickness of the depletion regions opening and closing the conduction channel. The fabrication process relies on strained III-V semiconductors which form a tubular shape upon selective releasing from the support substrates. The fabrication of the free-standing thin film transistors requires only conventional device patterning. Large area devices can thus be compacted to a footprint several orders of magnitude smaller than the planar counterpart. Our technique represents the ultimate limit of the bending radius of flexible inorganic thin film transistors.

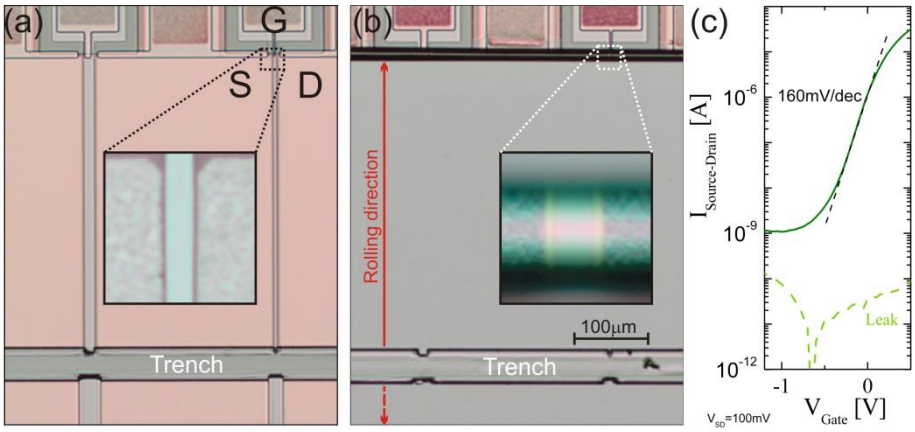

Figure 18. Inorganic thin film transistors (a) before and (b) after releasing and subsequent rolling-up. The insets are the magnified channel areas (15x15µm2). (c) The transfer characteristics shows a fast On-Off switching of 160mV/dec in the linear regime.

As a potential microfluidic application we demonstrate the possibility to sense solvents of different polarities. The liquids are injected via tiny glass capillaries at one end of the tube, over a millimeter away from the actual measurement region (Figure 19a). Due to the large capillary forces, the liquids are sucked into the hollow tube core towards the measurement region and can be detected by current changes. Sequential cycles of reproducible transfer characteristics are shown in Fig. 19(b) with a constant maximum current (dashed line). The injection of water leads to a current increase until reaching a saturation value ~100% higher. This effect can be explained by the change of the channel resistance due to variations of the surface potential. The adsorption of polar molecules on the surface results in a band bending, modifying the electron work function and the modified charge carrier density producing the sensing effect. This can be further verified by injection of liquids with different polarities. Fig. 19(c) shows the current variations during an injection sequence. Upon repeated injection of polar solvents (case 1, 3-4) the current increases substantially within seconds. After liquid removal, the current decreases exponentially down to the initial value. The polar solvents water, isopropanol C_3H_8O and tetrahydrofuran (THF) C_4H_8O as well as other investigated polar solvents such as ethanol C_2H_6O, acetone C_3H_6O, dimethylsulfoxide C_2H_6OS and dichloromethane CH_2Cl_2 (not shown) produce rapid current changes larger than 30µA. The good reproducibility of the sensing capabilities is demonstrated exemplarily by the repeated isopropanol injection (case 3) exhibiting similar current responses. As expected, no current variations can be detected for the non-polar n-hexane C_6H_{12} (case 2) and toluene C_7H_8 (not shown). The tubular transistor with a high sensitivity towards the polarity of physisorbed molecules may thus be integrated into microfluidic devices for future in-situ chemical and biological sensing applications.

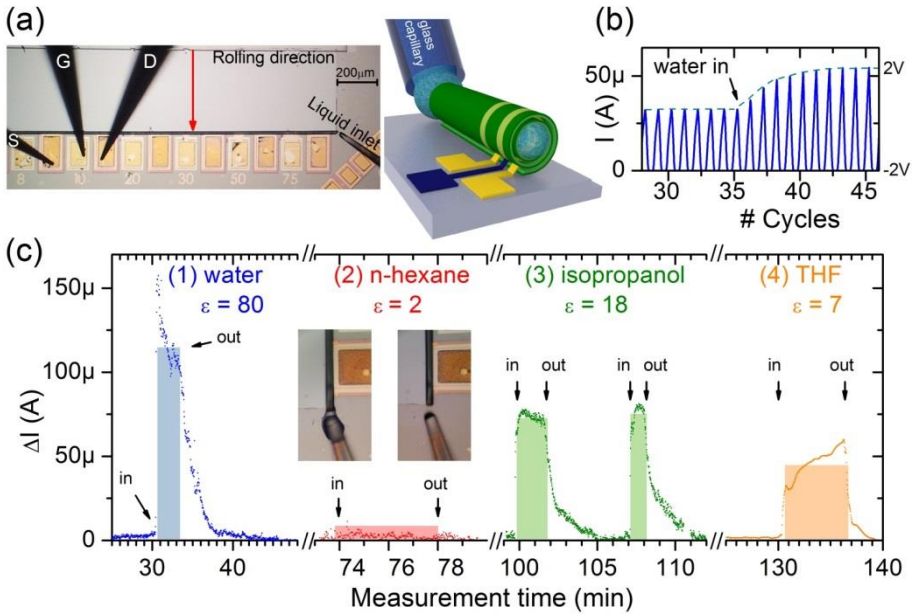

Figure 19. Chemical sensing of solvents with different polarities. (a) Experimental setup and sketch of the liquid injection in a probe station. (b) Cycled transfer characteristics (-2<Vg<2 V; VSD=0.1 V) during water injection. (c) Current variations as a function of measurement time upon exposure to solvents with different polarities. The liquid injections are indicated by shaded areas. Insets: Micrographs of tube-filling via tiny droplets.

Publications within project time:

1. S. Li, L. Ma, S. Böttner, Y. Mei, M. R. Jorgensen, S. Kiravittaya, O. G. Schmidt.
Angular position detection of single nanoparticles on rolled-up optical microcavities with lifted degeneracy
Phys. Rev. A 88, 033833, (2013)

2. S. Böttner, S. Li, M. R. Jorgensen, O. G. Schmidt.
Vertically aligned rolled-up SiO_2 optical microcavities in add-drop configuration
Appl. Phys. Lett. 102, 251119, (2013).

3. M. R. Jorgensen, S. Giudicatti, and O. G. Schmidt.
Diamond lattice photonic crystals from rolled-up membranes
Phys. Rev. A 87, 041803(R), (2013).

4. L. Ma, S. Li, V. A. Bolaños Quiñones, L. Yang, W. Xi, M. Jorgensen, S. Baunack, Y. Mei, S. Kiravittaya, O. G. Schmidt.
Dynamic molecular processes detected by microtubular opto-chemical sensors self-assembled from prestrained nanomembranes
Adv. Mater. 25, 2357, (2013).

5. D. Grimm, C. C. Bof Bufon, C. Deneke, P. Atkinson, D. J. Thurmer, F. Schäffel, S. Gorantla, A. Bachmatiuk, O. G. Schmidt.
Rolled-up nanomembranes as compact 3D architectures for field effect transistors and fluidic sensing applications
Nano Lett. 13, 213, (2013).

6. S. Böttner, S. L. Li, J. Trommer, S. Kiravittaya, O. G. Schmidt.
Sharp whispering-gallery modes in rolled-up vertical SiO2 microcavities with quality factors exceeding 5000
Opt. Lett. **37**, 5136 (2012).

7. S. M. Harazim, V. A. Bolaños Quiñones, S. Kiravittaya, S. Sanchez, O. G. Schmidt.
Lab-in-a-Tube: on-chip integration of glass optofluidic ring resonators for label-free sensing applications
Lab Chip, **12**, 2649 (2012). Cover Page: Lab Chip, **12**, 2587 (2012)

8. V. A. Bolaños Quiñones, L. Ma, S. Li, M. Jorgensen, S. Kiravittaya, O. G. Schmidt.
Enhanced optical axial confinement in asymmetric microtube cavities rolled up from circular-shaped nanomembranes
Opt. Lett. **37**, 4284 (2012) .

9. V. A. Bolaños Quiñones, L. Ma, S. Li, M. Jorgensen, S. Kiravittaya, O. G. Schmidt.
Localized optical resonances in low refractive index rolled-up microtube cavity for liquid-core optofluidic detection
Appl. Phys. Lett. **101**, 151107 (2012).

10. E. J. Smith, D. Makarov, O. G. Schmidt.
Polymer delamination: towards unique three-dimensional microstructures
Soft Matter **7**, 11309 (2011).

11. V. M. Fomin, E. J. Smith, D. Makarov, S. Sanchez, O. G. Schmidt.
Dynamics of radial-magnetized microhelix coils
Phys. Rev. B **84**, 174303 (2011).

12. E. J. Smith, S. Schulze, S. Kiravittaya, Y. F. Mei, S. Sanchez, O. G. Schmidt
Lab-in-a-tube: Detection of individual mouse cells for analysis in flexible split-wall microtube resonator sensors
Nano Lett. **10**, 4037 (2011).

13. L. B. Ma, S. Kiravittaya, V. A. Bolaños Quiñones, S. L. Li, Y. F. Mei, O. G. Schmidt.
Tuning of optical resonances in asymmetric microtube cavities
Opt. Lett. **36**, 3840 (2011).

14. E. J. Smith, D. Makarov, S. Sanchez, V. M. Fomin, O. G. Schmidt.
Magnetic microhelix coil structures
Phys. Rev. Lett. **107**, 097204 (2011).

15. E. J. Smith, Y. F. Mei, O. G. Schmidt.
Optical components for lab-in-a-tube systems
Proc. SPIE **8031**, 80310R (2011).

16. P. Cendula, S. Kiravittaya, I. Mönch, J. Schumann, O. G. Schmidt.
Directional roll-up of nanomembranes mediated by wrinkling
Nano Lett. **11**, 236 (2011).

17. Y. F. Mei, S. Kiravittaya, S. Harazim, O. G. Schmidt.

Principles and applications of micro and nanoscale wrinkles
Mater. Sci. Eng. R **70**, 209 (2010).

18. H.-X. Ji, X.-L. Wu, L.-Z. Fan, C. Krien, I. Fiering, Y.-G. Guo, Y. F. Mei, O. G. Schmidt.
Self-wound composite nanomembranes as electrode materials for lithium ion batteries
Adv. Mater. **22**, 4591 (2010).

19. P. Feng, I. Mönch, G. S. Huang, S. Harazim, E. J. Smith, Y. F. Mei, O. G. Schmidt.
Local-illuminated ultrathin silicon nanomembranes with photovoltaic effect and negative transconductance
Adv. Mater. **22**, 3667 (2010).

20. C. C. Bof Bufon, J. D. C. Gonzlez, D. J. Thurmer, D. Grimm, M. Bauer, O. G. Schmidt.
Self-assembled ultra-compact energy storage elements based on hybrid nanomembranes
Nano Lett. **10**, 2506 (2010).

21. G. S. Huang, V. A. Bolaños Quiñones, F. Ding, S. Kiravittaya, Y. F. Mei, O. G. Schmidt.
Rolled-up optical microcavities with subwavelength wall thicknesses for enhanced liquid sensing applications
ACS Nano **4**, 3123 (2010).

22. H. X. Ji, Y. F. Mei, O. G. Schmidt.
Swiss roll nanomembranes with controlled proton diffusion as redox micro-supercapacitors
Chem. Commun. **46**, 3881 (2010).